

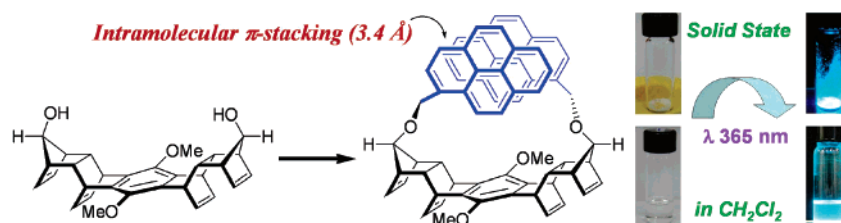
## Bicyclo[2.2.2]octene-Based “Crab-like” Molecules: Synthesis, Complexation, Luminescence Properties, and Solid-State Structures

Teh-Chang Chou,\* Ching-Lun Hwa, Jin-Ju Lin, Kung-Ching Liao, and Jui-Chang Tseng

Department of Chemistry and Biochemistry, National Chung Cheng University, Minshong, Chiayi 621, Taiwan

chetcc@ccu.edu.tw

Received May 20, 2005



The U-shaped, multifunctionalized tetraetheno-bridged dicyclopenta[*b,i*]anthracenediol **10** was synthesized to serve as a platform molecule. The molecule was prepared from the Diels–Alder adduct **5a** of tricycloundecatriene **3** and bicyclo[2.2.2]octene-fused *p*-benzoquinone **4**. Functionalization of **10** to construct crab-like molecules was achieved via the base-promoted bis-*O*-alkylation of two endo-oriented hydroxyl groups at termini in **10** with the following alkyl halides: allyl, propargyl, and benzyl bromides; 1-bromo- and 1-iodo-4-(bromomethyl)benzene; 9-(bromomethyl)anthracene; 1-(bromomethyl)pyrene; and isomeric bromomethylpyridines. Single-crystal X-ray structures were obtained for bis-phenyl (**21**) and bis-pyrenyl (**25**) crabs, and for the silver(I) complex (**32** and **33**) crabs. The silver(I) complex **32** from bis-*o*-pyridyl crab **30** is a [2+2] dimeric dimetalocyclophane, and **33** from bis-*m*-pyridyl crab **29** is a [1+1] metallo-bridged cyclophane. The self-assembled intramolecular  $\pi$ -stacking of pyrenyl rings in **25** with an interplanar distance of 3.40 Å and the consequent  $\pi$ – $\pi$  interactions were revealed by the X-ray crystal structure and its luminescence property.

### Introduction

The synthetic endeavor toward polycyclic molecules of specially designed architecture has been actively demonstrated in the search for new chemical species that may effectively form more highly organized structure systems (supermolecules) of biological and practical importance.<sup>1</sup> To attain such chemical species, researchers frequently utilize rigid and often symmetric polycarbocyclic skeletons to serve as “platforms” for the attachment of functional groups or ligands that are capable of forming

the covalent or coordinative metal–ligand bonds,<sup>2</sup> or for operating the noncovalent intermolecular interactions, such as hydrogen bonding, ion-pairing, and arene–arene interactions, in the processes of molecular recognition and self-assembly.<sup>3</sup> A variety of smaller molecules have been utilized to serve as basic building blocks for constructing polycarbocyclic platform molecules. Among the most notable examples are bicyclo[2.2.1]heptane (norbornane) and/or 7-oxabicyclo[2.2.1]heptane rings adopted by the

(1) (a) Hosseini, M. W. *Acc. Chem. Res.* **2005**, *38*, 313–323. (b) Lee, S.; Mallik, A. B.; Xu, Z.; Lobkovsky, E. B.; Tran, L. *Acc. Chem. Res.* **2005**, *38*, 251–261. (c) Boyd, P. D. W.; Reed, C. A. *Acc. Chem. Res.* **2005**, *38*, 235–242. (d) Sakai, N.; Mareda, J.; Matile, S. *Acc. Chem. Res.* **2005**, *38*, 79–87. (e) Cantrill, S. J.; Chichak, K. S.; Peters, A. J.; Stoddart, J. F. *Acc. Chem. Res.* **2005**, *38*, 1–9. (f) Meyer, E. A.; Castellano, R. K.; Diederich, F. *Angew. Chem., Int. Ed.* **2003**, *42*, 1210–1250. (g) Leininger, S.; Olenyuk, B.; Stang, P. *Chem. Rev.* **2000**, *100*, 853–908. (h) Lehn, J. M. *Supramolecular Chemistry: Concept and Perspectives*; VCH: Weinheim, Germany, 1995.

(2) (a) Seidel, S. R.; Stang, P. J. *Acc. Chem. Res.* **2002**, *35*, 972–983. (b) Swieggers, G. F.; Malefetse, T. J. *Chem. Rev.* **2000**, *100*, 3483–3538. (c) Michl, J. *Chem. Rev.* **1999**, *99*, 1863–1933. (d) Schultz, A. C.; Kelso, L. S.; Johnston, M. R.; Warrenner, R. N.; Keene, F. R. *Inorg. Chem.* **1999**, *38*, 4908–4909.

(3) (a) Harmata, M. *Acc. Chem. Res.* **2004**, *37*, 862–873. (b) Hof, F.; Craig, S. L.; Nuckolls, C.; Rebek, J. *Angew. Chem., Int. Ed.* **2002**, *41*, 1488–1508. (c) Nemoto, H.; Kawano, T.; Ueji, N.; Bando, M.; Kido, M.; Suzuki, I.; Shibuya, M. *Org. Lett.* **2000**, *2*, 1015–1017. (d) Potluri, V. K.; Maitra, U. J. *Org. Chem.* **2000**, *65*, 7764–7769. (e) D’Souza, L. J.; Maitra, U. J. *Org. Chem.* **1996**, *61*, 9494–9502. (f) Ma, J. C.; Dougherty, D. A. *Chem. Rev.* **1997**, *97*, 1303–1324.

groups of Zimmt<sup>4</sup> and Paddon-Row<sup>5</sup> to construct donor–spacer–acceptor systems for the study of long-range electron and energy-transfer phenomena, by Warrenner<sup>6</sup> and Klärner<sup>7</sup> to build the U-shaped molecular clefts, tweezers, and clips to act as host molecules, and by Stoddart<sup>8</sup> to design a molecular “LEGO” for the assembly of molecular belts.

However, we have been interested in the polycyclic systems that are constructed with the bicyclo[2.2.2]octene (abbreviated as BCO) ring as the major building block, in which all the etheno-bridge double bonds are positioned on the same face of the carbon skeleton, as illustrated by the generic structure **A** and the corresponding graphic representation (Figure 1). In rack-shaped polyenes of system **A**, which we have successfully demonstrated in several reports,<sup>9</sup> all the proximate bridge double bonds are syn-facially arranged and separated by an internuclear distance of ca. 2.9 Å for effective laticyclic conjugation,<sup>10</sup> and are taken into account for the facile

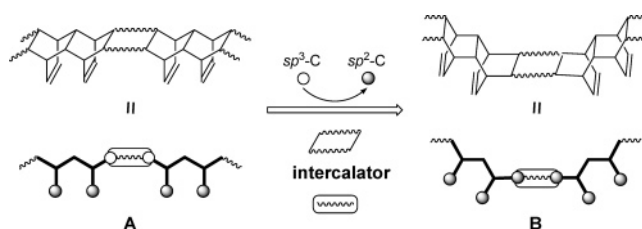


**FIGURE 1.** Schematic representations of the syn-facial etheno-bridged bicyclo[2.2.2]octene-based polyenes, and the change of shape upon alteration of the intercalator from  $sp^3$ -C type to  $sp^2$ -C type.

transannular ring formation via electrophilic addition reactions<sup>9,11</sup> and [2+2] photocyclization.<sup>9,12,13</sup> A spacer is used to couple the BCO rings by Diels–Alder reaction, and can be tailored to control the molecular length, shape, and configuration. For example, as illustrated in Figure 1, the rack-shaped polyene with a boat-form cyclohexane ring as an intercalator ( $sp^3$ -C junction, **A**) can be altered to take a U-shaped framework by changing to a planar benzene-ring connector ( $sp^2$ -C junction, **B**).<sup>13a</sup> With such a change in the intercalator as such, a concave space between two termini is created in polyenes of type **B**, which could then serve as a platform, via further elaboration at both termini of the polycyclic framework, for the synthesis of specially designed molecules, such as clefts, tweezers, and belts.

Synthetic approaches toward polycyclic polyenes of types **A** and **B** require good stereoselective control on the configuration at each ring junction (cis-fused) and the orientation of all etheno-bridges of the BCO rings (syn-facial). To achieve such stereoselective synthesis, we adopted the Diels–Alder reaction as the key reaction. We prepared the BCO-fused *p*-benzoquinone **4**,<sup>13</sup> as outlined in Scheme 1, from readily available 1,2,3,4-tetrachloro-5,5-dimethoxycyclopentadiene (**1**)<sup>14</sup> and *p*-benzoquinone (**2**) via pivotal intermediate tricycloundecatriene **3**, which we considered as a synthetic equivalent of *cis*-9,10-dihydronaphthalene (the masked *cis*-DHN).<sup>15</sup> Because of its curved-in configuration, the masked *cis*-DHN **3** un-

(4) (a) Troisi, A.; Ratner, M. A.; Zimmt, M. B. *J. Am. Chem. Soc.* **2004**, *126*, 2215–2224. (b) Nadeau, J. M.; Liu, M.; Waldeck, D. H.; Zimmt, M. B. *J. Am. Chem. Soc.* **2003**, *125*, 15964–15973. (c) Zimmt, M. B.; Waldeck, D. H. *J. Phys. Chem. A* **2003**, *107*, 3580–3597. (d) Napper, A. M.; Read, I.; Kaplan, R.; Zimmt, M. B.; Waldeck, D. H. *J. Phys. Chem. A* **2002**, *106*, 5288–5296. (e) Napper, A. M.; Read, I.; Waldeck, D. H.; Kaplan, R.; Zimmt, M. B. *J. Phys. Chem. A* **2002**, *106*, 4784–4793. (f) Kaplan, R.; Napper, A. M.; Waldeck, D. H.; Zimmt, M. B. *J. Phys. Chem. A* **2002**, *106*, 1917–1925.

(5) (a) Napper, A. M.; Head, N. J.; Oliver, A. M.; Shephard, M. J.; Paddon-Row, M. N.; Read, I.; Waldeck, D. H. *J. Am. Chem. Soc.* **2002**, *124*, 10171–10181. (b) Bell, T. D. M.; Ghiggino, K. P.; Jolliffe, K. A.; Ranasinghe, M. G.; Shephard, M. J.; Langford, S. J.; Paddon-Row, M. N. *J. Phys. Chem. A* **2002**, *106*, 10079–10088. (c) Smith, T. A.; Lokan, N.; Cabral, N.; Davies, S. R.; Paddon-Row, M. N.; Ghiggino, K. P. *J. Photochem. Photobiol. A* **2002**, *149*, 55–69. (d) Bell, T. D. M.; Jolliffe, K. A.; Ghiggino, K. P.; Oliver, A. M.; Shephard, M. J.; Langford, S. J.; Paddon-Row, M. N. *J. Am. Chem. Soc.* **2000**, *122*, 10661–10666. (e) Napper, A. M.; Read, I.; Waldeck, D. H.; Head, N. J.; Oliver, A. M.; Paddon-Row, M. N. *J. Am. Chem. Soc.* **2000**, *122*, 5220–5221. (f) Lokan, N. R.; Paddon-Row, M. N.; Koeberg, M.; Verhoeven, J. W. *J. Am. Chem. Soc.* **2000**, *122*, 5075–5081. (g) Head, N. J.; Oliver, A. M.; Look, K.; Lokan, N. R.; Jones, G. A.; Paddon-Row, M. N. *Angew. Chem., Int. Ed.* **1999**, *38*, 3219–3222. (h) Paddon-Row, M. N. *Acc. Chem. Res.* **1994**, *27*, 18–25.

(6) (a) Johnston, M. R.; Latter, M. J.; Warrenner, R. N. *Org. Lett.* **2002**, *4*, 2165–2168. (b) Butler, D. N.; Shang, M.; Warrenner, R. N. *Chem. Commun.* **2001**, 159–160. (c) Warrenner, R. N.; Margetic, D.; Foley, P. J.; Butler, D. N.; Winling, A.; Beales, K. A.; Russell, R. A. *Tetrahedron* **2001**, *57*, 571–582. (d) Warrenner, R. N.; Margetic, D.; Amarasekara, A. S.; Russell, R. A. *Org. Lett.* **1999**, *1*, 203–206. (e) Warrenner, R. N.; Butler, D. N.; Russell, R. A. *Synlett* **1998**, 566–573. (f) Warrenner, R. N.; Margetic, D.; Amarasekara, A. S.; Butler, D. N.; Mahadevan, I. B.; Russell, R. A. *Org. Lett.* **1999**, *1*, 199–202.

(7) (a) Klärner, F. G.; Kahlert, B.; Boese, R.; Bläser, D.; Juris, A.; Marchioni, F. *Chem.–Eur. J.* **2005**, *11*, 3363–3374. (b) Fokkens, M.; Jasper, C.; Schrader, T.; Kozioł, F.; Ochsenfeld, C.; Polkowska, J.; Lobert, M.; Kahlert, B.; Klärner, F. G. *Chem.–Eur. J.* **2005**, *11*, 477–494. (c) Schalley, C. A.; Verhaelen, C.; Klärner, F. G.; Hahn, U.; Vögtle, F. *Angew. Chem., Int. Ed.* **2005**, *44*, 477–480. (d) Klärner, F. G.; Polkowska, J.; Panitzky, J.; Seelbach, U. P.; Burkert, U.; Kamieth, M.; Baumann, M.; Wigger, A. E.; Boese, R.; Bläser, D. *Eur. J. Org. Chem.* **2004**, 1405–1423. (e) Klärner, F.-G.; Kahlert, B. *Acc. Chem. Res.* **2003**, *36*, 919–932. (f) Klärner, F.-G.; Lobert, M.; Naatz, U.; Bandmann, H.; Boese, R. *Chem.–Eur. J.* **2003**, *9*, 5036–5047. (g) Klärner, F.-G.; Panitzky, J.; Bläser, D.; Boese, R. *Tetrahedron* **2001**, *57*, 3673–3687. (h) Klärner, F.-G.; Burkert, U.; Kamieth, M.; Boese, R. *J. Phys. Org. Chem.* **2000**, *13*, 604–611. (i) Klärner, F.-G.; Burkert, U.; Kamieth, M.; Boese, R.; Benet-Buchholz, J. *Chem.–Eur. J.* **1999**, *5*, 1700–1707. (j) Kamieth, M.; Burkert, U.; Corbin, P. S.; Dell, S. J.; Zimmerman, S. C.; Klärner, F.-G. *Eur. J. Org. Chem.* **1999**, 2741–2749. (k) Kamieth, M.; Klärner, F.-G.; Diederich, F. *Angew. Chem., Int. Ed.* **1998**, *37*, 3303–3306.

(8) (a) Philip, D.; Stoddart, J. F. *Angew. Chem., Int. Ed.* **1996**, *35*, 1155–1196. (b) Ashton, P. R.; Brown, G. R.; Isaacs, N. S.; Gluffrida, D.; Kohnke, F. H.; Mathias, J. P.; Slawin, A. M. Z.; Smith, D. R.; Stoddart, J. F.; Williams, D. J. *J. Am. Chem. Soc.* **1992**, *114*, 6330–6353. (c) Mathias, J. P.; Stoddart, J. F. *Chem. Soc. Rev.* **1992**, 215–225.

(9) (a) Lin, C.-T.; Chen, K.-Z.; Chou, T.-C. *Tetrahedron* **2003**, *59*, 1493–1500. (b) Chou, T.-C.; Kuo, L.-H.; Liu, K.-F. *J. Chin. Chem. Soc.* **2003**, *50*, 303–312. (c) Lin, C.-T.; Hsu, H.-C.; Wang, M.-F.; Chou, T.-C. *Tetrahedron* **2000**, *56*, 5383–5390. (d) Lin, C.-T.; Hsu, H.-C.; Chou, T.-C. *J. Org. Chem.* **1999**, *64*, 7260–7264. (e) Chou, T.-C.; Jiang, T.-S.; Hwang, J.-T.; Lin, K.-J.; Lin, C.-T. *J. Org. Chem.* **1999**, *64*, 4874–4883.

(10) Goldstein, M. J.; Hoffmann, R. *J. Am. Chem. Soc.* **1971**, *93*, 6193–6204.

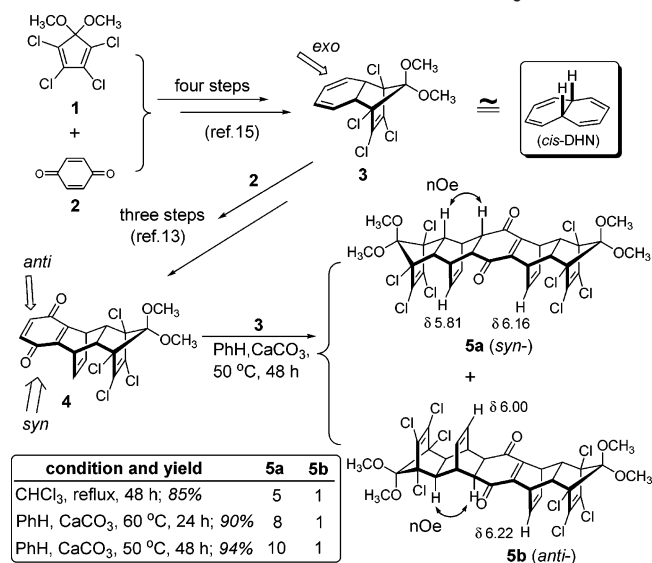
(11) (a) Lee, C.-H.; Liang, S.; Haumann, T.; Boese, R.; de Meijere, A. *Angew. Chem., Int. Ed.* **1993**, *32*, 559–561. (b) Kimura, M.; Morosawa, S. *J. Org. Chem.* **1985**, *50*, 1532–1534. (c) Ōsawa, E.; Aigami, K.; Inamoto, Y. *Tetrahedron* **1978**, *34*, 509–515.

(12) (a) Metha, G.; Padma, S.; Ōsawa, E.; Barbiric, D. A.; Mochizuki, Y. *Tetrahedron Lett.* **1987**, *28*, 1295–1298. (b) Ōsawa, E.; Aigami, K.; Inamoto, Y. *Tetrahedron* **1978**, *34*, 509–515. (c) Ōsawa, E.; Aigami, K.; Inamoto, Y. *J. Org. Chem.* **1977**, *42*, 2621–2626. (d) Eaton, P. E.; Cassar, L.; Hudson, R. A.; Hwang, D. R. *J. Org. Chem.* **1976**, *41*, 1445–1448. (e) Marchand, A. P.; Chou, T.-C.; Ekstrand, J. D.; van der Helm, D. *J. Org. Chem.* **1976**, *41*, 1438–1444. (f) Smith, E. C.; Barborak, J. C. *J. Org. Chem.* **1976**, *41*, 1433–1437.

(13) (a) Chou, T.-C.; Lin, G.-H. *Tetrahedron* **2004**, *60*, 7907–7920. (b) Marchand, A. P.; Alihodzic, S.; Shukla, R. *Synth. Commun.* **1998**, *28*, 541–546.

(14) (a) Khan, F. A.; Prabhudas, B.; Dash, J. *J. Prakt. Chem.* **2000**, *342*, 512–517. (b) Ungnade, H. E.; McBee, E. T. *Chem. Rev.* **1958**, *58*, 249–320. (c) Newcomer, J. S.; McBee, E. T. *J. Am. Chem. Soc.* **1949**, *71*, 946–951.

(15) (a) Forman, M. A.; Dailey, W. P. *J. Org. Chem.* **1993**, *58*, 1501. (b) Chou, T.-C.; Chiou, J.-H. *J. Chin. Chem. Soc.* **1986**, *33*, 227–234.

**SCHEME 1. Preparation and Diels–Alder Reaction of the Masked *cis*-DHN 3 and Quinone 4**


derwent the Diels–Alder reactions via exclusive attack of the dienophile upon the exo face of the diene to give a single adduct, in which the newly formed double bond of the BCO substructure is disposed in parallel with and in proximity to the chlorine-substituted double bond.<sup>9,16</sup> The environment between the *p*-benzoquinone unit and the etheno-bridge in quinone 4 (defined as syn face) is sterically less inhibited, such that the more favorable syn-facial attack of the diene upon the enedione moiety of 4 was expected and realized.<sup>13a</sup> Consequently, we anticipated the Diels–Alder reaction of the masked *cis*-DHN 3 and quinone 4 to follow the same stereoselective preference and exhibit high  $\pi$ -facial selectivity, yielding a bis-adduct of desired stereochemistry. Indeed as expected, quinone 4 underwent the Diels–Alder reaction with the masked *cis*-DHN 3 stereoselectively to furnish 5a, the adduct of desired stereochemistry as the major product (Scheme 1).<sup>17</sup>

Adduct 5a is the common precursor toward the polycyclic polyene systems of either type A or B by the alteration of the intercalator. The type A systems can be attained by hydrogenation of the enedione moiety using McMurry's procedure,<sup>17</sup> and the type B systems via aromatization employing the enolization process.<sup>13a</sup> The latter endeavor led us to prepare tetraetheno-bridged dicyclopenta[*b,i*]anthracenediol 10. Diol 10 is a U-shaped, multifunctionalized platform molecule, which holds two endo-oriented hydroxyl groups at termini that are suitable for the attachment of functional groups or ligands—resembling the pair of pincers of a crab—via reactions such as bis-*O*-alkylation with alkyl halides (Figure 2). In this paper, we describe the synthesis of platform molecule 10 and the construction of the "crab-like"

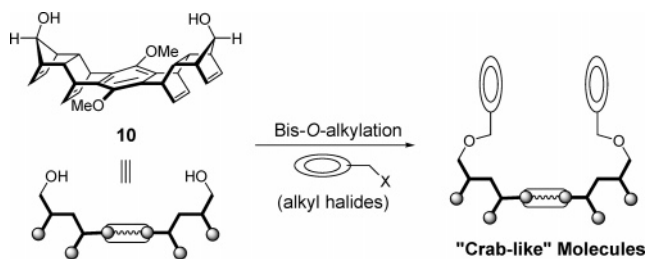


**FIGURE 2.** Construction of molecular crabs via bis-*O*-alkylation of dicyclopenta[*b,i*]anthracenediol 10.

molecules, whose concave, pincer-like nature and arene–arene interactions were revealed by X-ray crystallography, complexation, and luminescence properties.

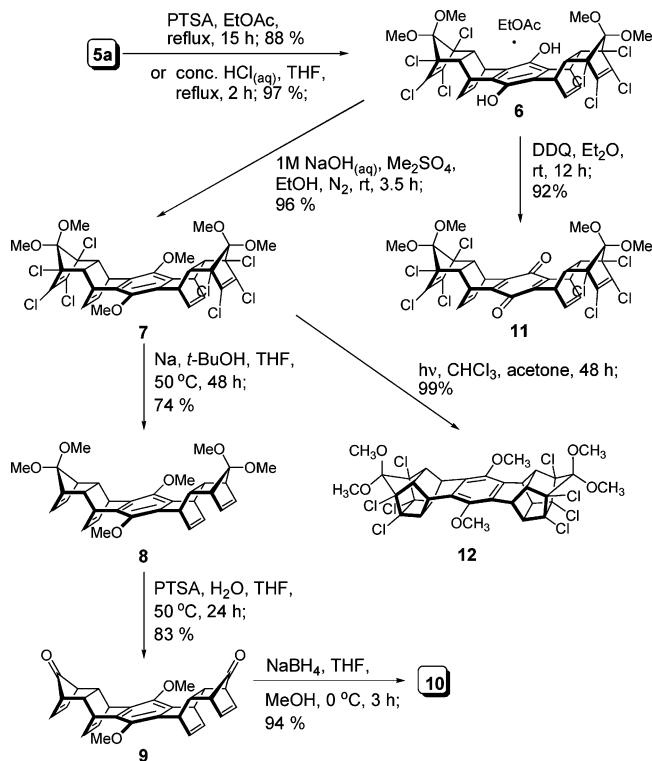
**Results and Discussion**

**Synthesis of Platform Molecule 10.** The bicyclo[2.2.2]octadiene-fused *p*-benzoquinone 4 is  $\pi$ -facially dissymmetric, as is the masked *cis*-DHN 3. In principle, eight modes of the Diels–Alder reaction of 3 and 4 leading to eight stereoisomeric adducts are possible, taking into account the endo/exo selectivity (the alignment of the two reacting components in the transition state interpreted by the Alder rule) and the  $\pi$ -facial selectivity ( $\pi$ -face on which bond formation is taking place). However, it seems reasonable to expect that the Diels–Alder reaction of 4 with the masked *cis*-DHN 3 via the anti-Alder modes of cycloaddition would lead to transition states of higher energy because of the disfavored steric interactions between two reacting components that are aligned in parallel with each other. Together with the fact that the masked *cis*-DHN 3, though  $\pi$ -facially dissymmetric, can offer only one of its  $\pi$ -faces (exo-face) for cycloaddition,<sup>9,16</sup> the modes of the Diels–Alder reaction of 3 and 4 would therefore be reduced to only two. These are the additions that occur in accordance with the Alder's endo-rule, thereby producing two products, syn- and anti-adduct. Experimentally, as shown in Scheme 1,<sup>17</sup> when a solution of 3 and 4 in chloroform was refluxed for 2 days, the Diels–Alder reaction produced two adducts in a ratio of 5:1. The ratio of these two products was increased to 8:1 when the reaction was performed by heating the reaction mixture at 60 °C in the presence of CaCO<sub>3</sub> (1 equiv) using less polar benzene as solvent, and could be further enhanced to 10:1 (94% total yield) by lowering the reaction temperature to 50 °C. Both adducts resulted from the modes of addition of 3 via the exo-approach at the periphery activated double bond of 4 in accordance with the Alder's endo-rule as supported by the NOESY spectral analysis, which revealed the interactions between the hydrogens at carbons  $\alpha$  to the carbonyl groups and the methine hydrogens at the junction of bicyclic rings. The major adduct was assigned to be the syn-adduct 5a based on the <sup>1</sup>H NMR spectrum, in which the absorption signals for the vinyl hydrogens of the BCO moieties appeared at  $\delta$  6.16 and 5.81, upfield shifts relative to those of anti-adduct 5b ( $\delta$  6.22 and 6.00). This upfield shift is attributed to the consequence of the anisotropic shielding effect on vinyl hydrogens by the face-to-face juxtaposed double bond across the cyclohexenedione ring in 5a, and is well-demonstrated in other

(16) The fact that the masked *cis*-DHN 1 can offer only one of its  $\pi$ -faces (exo-face) for DA reaction, thereby generating two facially proximate and well-aligned double bonds, is supported by the isolation of the single adduct and subsequent conversion of it to the corresponding cage compound by the [2+2] photocyclization: Chou, T.-C.; Chuang, K.-S.; Lin, C.-T. *J. Org. Chem.* **1988**, *53*, 5168–5170.

(17) (a) Tseng, J.-C. M.S. Thesis, National Chung Cheng University, 1999. (b) Chin, H.-C. M.S. Thesis, National Chung Cheng University, 1995.



**SCHEME 2. Synthesis of Tetraetheno-Bridged Dicyclopenta[*b,i*]anthracenediol 10**


similar compounds reported<sup>18</sup> and prepared in this laboratory.<sup>9,13a</sup>

Because tetraalkyl-substituted hydroquinones and especially the corresponding anions are prone to oxidation, aromatization of **5a** to the corresponding hydroquinone via the enolization process was carried out in acidic conditions. Thus, as illustrated in Scheme 2, acid-catalyzed enolization of **5a** went smoothly to give hydroquinone **6**, which was characterized as complex **EtOAc@6**. The reasons for this were that (1) the removal of the encapsulated molecule of EtOAc from **EtOAc@6** proved to be rather difficult, so that even sublimation was not effectively useful; and (2) without entrapped EtOAc in either solution or solid form, the hydroquinone moiety in **6** was found to be oxidized to a quinone structure within a few days upon exposure to air, giving the corresponding light-sensitive quinone **11**. Quinone **11** could also be obtained in 92% yield via oxidation with DDQ in ether. In solid state as shown by the X-ray crystal structure (Figure 3), a molecule of EtOAc is entrapped in the cavity of **6** with its methyl group embedded by inward methoxyl groups of **6**, and its top capped by another molecule of **6** (Figure S16, Supporting Information) supported by intermolecular hydrogen bonding between the carbonyl oxygen of EtOAc and the hydroxyl hydrogen atom of **6** ( $d_{O\cdots H} = 1.85 \text{ \AA}$ ). The central dihydroxybenzene ring-containing platform is not totally flat, but slightly twisted and inward-folded by a total of about  $5.1^\circ$ . The consequently affected transannular distances between oxygen atoms (O1–O2') of inward methoxyl groups, methano-bridge carbon atoms (C1–C1'), and ring

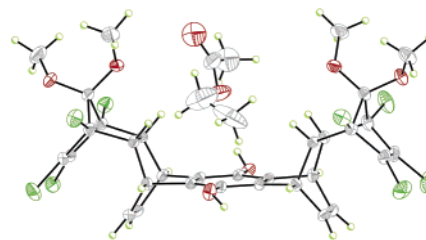


**FIGURE 3.** ORTEP drawing of **EtOAc@6**. The thermal ellipsoids are drawn at the 30% level of probability. There are four molecules of **EtOAc@6** in a unit cell. The hydrogen bond formed by the carbonyl oxygen of EtOAc and the hydroxy hydrogen atom of another molecule of **6** (not shown) is 1.85 Å long.

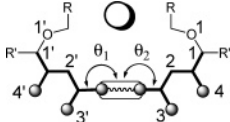
junction carbon atoms (C2–C2') are 7.62, 9.59, and 6.32 Å, respectively (Table 1). These distances are taken to define the cavity dimension of the U-shaped scaffold of **6**. All the etheno-bridges are located syn-facially on the convex side of the carbon scaffold, and the two pairs of etheno-bridges are separated by 6.75 Å. The distance between the paired etheno-bridges is about 2.95 Å.

Preliminary investigation indicated that the reductive dechlorination **6** yielded the corresponding hydroquinone, which was always contaminated by various amounts of yellow-colored benzoquinone resulting from the air-oxidation of hydroquinone. Therefore, hydroquinone **6** was converted to the dimethoxybenzene derivative **7** via bis-*O*-methylation prior to the reductive dechlorination process. To minimize the accumulation of base-generated hydroquinone anions, and thus the concomitant formation of quinone **11**, we performed the bis-*O*-methylation with dropwise addition of an aqueous NaOH solution to a mixture of **6** and dimethyl sulfate in EtOH under a N<sub>2</sub> atmosphere. The dimethoxybenzene derivative **7** thereby obtained in 96% yield was subsequently subjected to the reductive dechlorination with sodium shot and *tert*-butyl alcohol in anhydrous THF ( $\rightarrow$  **8**, 74%), followed by PTSA-catalyzed deketalization of **8** at 50 °C to give thermally and photochemically labile dione **9** (83% yield).<sup>19</sup> Reduction of dione **9** in MeOH with NaBH<sub>4</sub> at 0 °C, using THF as a cosolvent to circumvent the solubility problem, furnished the targeted endo,endo-diol **10** in a yield of 94% without concomitant formation of other stereoisomers (exo,exo- or exo,endo-diol). To demonstrate the proximity of the face-to-face juxtaposed etheno-bridge double bonds in these BCO-based polycyclic polyenes, which is also indicated by the upfield shifts of <sup>1</sup>H absorption signals for etheno-bridge hydrogens ( $\delta$  5.6–5.9) because of a mutual anisotropic shielding effect,<sup>13a,18</sup> a solution of tetraene **7** in CHCl<sub>3</sub> was subjected to the acetone-sensitized irradiation (acetone:CHCl<sub>3</sub> = 1:1;  $\lambda = 254 \text{ nm}$ ). The [2+2] photocyclized double-caged compound **12** was obtained in quantitative yield (Scheme 2).

Diol **10**, mp 262–263 °C, shows an infrared absorption band at 3361 cm<sup>-1</sup> due to hydroxyl groups. It is C<sub>2v</sub>-symmetric, as were its precursors, exhibiting nine ab-

(18) This kind of consequence is typical for *endo,endo*-dimethanonaphthalene and other related homologous systems: Astin, K. B.; Mackenzie, K. *J. Chem. Soc., Perkin Trans. 2* **1975**, 1004–1010.

(19) The decarbonylation of dione **9** followed by the fragmentation via retro-Diels–Alder reaction to completely form benzene and 9,10-dimethoxyanthracene was observed in THF under reflux for a few hours or in a transparent bottle for half a year. The reactions are characteristic of bicyclo[2.2.1]hepta-2-ene-7-one and 1,4,4a,8a-tetrahydro-1,4-ethenonaphthalene systems: Birney, D. M.; Berson, J. A. *Tetrahedron* **1986**, *42*, 1561–1570.

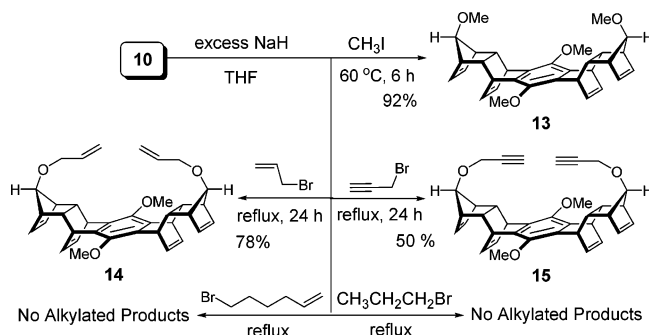
**TABLE 1.** Selected Interatomic Distances (Å) and Torsional Angles ( $\theta$ , Deg) in the Crystal Structures of Molecular Crabs **6**, **21**, **25**, and **33**


compd	O1–O1'	C1–C1'	C2–C2' <sup>a</sup>	C3–C3' <sup>a</sup>	C3–C4 <sup>a</sup>	C3'–C4 <sup>a</sup>	$\theta_1^a$	$\theta_2^a$
<b>6</b>	7.62	9.59	6.27	6.75	2.96	2.94	176.8	178.7
<b>21</b>	7.06	9.10	6.05	6.96	2.98	2.97	176.6	174.1
<b>25</b>	7.57	9.46	6.23	6.83	2.97	2.98	176.5	176.4
<b>33<sup>b</sup></b>	7.62	9.59	6.27	6.75	2.96	2.94	176.8	178.7

**6** R: H; R': -OCH<sub>3</sub>; ○: AcOEt  
**21** R: phenyl; R': H; ○: ---  
**25** R: Pyren-1-yl; R': H; ○: ---  
**33** R: Pyrid-3-yl; R': H; ○: Ag<sup>+</sup>

<sup>a</sup> Average of two values. <sup>b</sup> N–Ag average distance 2.16 Å; N–Ag–N' endocyclic angle 174.8°.

### SCHEME 3. Bis-*O*-Alkylation of Diol **10** with Methyl, Allyl, Propargyl, Propyl, and Hex-1-en-6-yl Halides



sorption lines in the broadband-decoupled <sup>13</sup>C NMR spectrum for 30 carbons and eight groups of proton signals for 30 hydrogens in the <sup>1</sup>H NMR spectrum. The endo,endo-oriented stereochemistry of two hydroxyl groups in **10** is suggested by the course of reduction, in which the hydride species approaches the carbonyl groups from the sterically less-hindered convex side (syn to the double bond) of dione **9**, and is supported by the pertinent precedents of the hydride reductions of simpler 7-norbornenone derivatives.<sup>20</sup> The stereochemical assignment of diol **10** is further secured by the comparison of the chemical shift of the newly introduced bridge protons geminal to the hydroxyl group in **10** ( $\delta$  3.59) with those of the same proton in *anti*-7-norbornenol ( $\delta$  3.53) and its syn isomer ( $\delta$  3.31),<sup>21</sup> and becomes manifest in the later stage of synthesis.

**Synthesis of the Molecular Crabs.** With acquisition of endo,endo-diol **10**, we embarked on the construction of molecular crabs via bis-*O*-alkylation using the methodology similar to Williamson ether synthesis. At the outset, considering the bis-*O*-alkylations to occur in the sterically unfavorable concave space of U-shaped diol **10**, the reactions were performed by treatment of **10** with excess NaH at 60 °C or refluxing temperature of THF in the presence of excess simple alkylating agents, and the results are outlined in Scheme 3. With methyl iodide, allyl bromide, and propargyl bromide as alkylating agents, the reaction furnished the bis-*O*-alkylated products **13**,

**14**, and **15** in 92, 78, and 50% yields, respectively. However, we were unable to obtain the corresponding alkylated products of **10** with *n*-propyl bromide and 6-bromohex-1-ene. Presumably, alkyl halides that are susceptible to a base-induced 1,2-elimination underwent such a reaction more rapidly than substitution under these conditions. We also observed that the alkoxide ions derived from diol **10** began to show thermal instability at 60 °C. To minimize the base-promoted decomposition of diol **10**, we thus operated the bis-*O*-alkylations at 45 °C by preparing a THF solution of alkylating agent (3 equiv) in the presence of excess NaH (10 equiv) followed by adding diol **10**, and the reactions usually took 2–5 days to complete. In this manner, we performed the bis-*O*-alkylation reactions of diol **10** with the following arylmethyl bromides: benzyl bromide (**16**), 1-bromo-4-(bromomethyl)benzene (**17**), 1-iodo-4-(bromomethyl)benzene (**18**), 9-(bromomethyl)anthracene (**19**),<sup>22</sup> and 1-(bromomethyl)pyrene (**20**).<sup>23</sup> The anthracenyl<sup>24</sup> and pyrenyl ring-appended<sup>25</sup> alkylating agents (**19** and **20**) were chosen for examining chromogenic and fluorogenic behavior, and possible intra- and/or intermolecular  $\pi$ – $\pi$  orbital interactions of the resulting bis-arylmethyl ethers **24** and **25**, particularly the consequences of  $\pi$ -stacking of aryl rings in their solid-state structures.<sup>26</sup> As shown in Scheme 4, we were able to prepare the bis-arylmethyl ethers **21**–**25** in satisfactory yields, ranging from 60 to 85%.

Encouraged by the synthetic implementation shown in Scheme 4, we extended our work to incorporate pyridylmethyl groups to the polycyclic framework of diol **10**. The

(20) (a) Yadav, V. K.; Balamurugan, R. *J. Org. Chem.* **2002**, *67*, 587–590. (b) Mehta, G.; Gagliardini, V.; Priyakumar, U. D.; Sastry, G. N. *Tetrahedron Lett.* **2002**, *43*, 2487–2490. (c) Mehta, G.; Khan, F. A. *Tetrahedron Lett.* **1992**, *33*, 3065–3068. (d) Paquette, L. A.; Dunkin, I. R. *J. Am. Chem. Soc.* **1975**, *97*, 2243–2249.

(21) Synder, E. I.; Franzus, B. *J. Am. Chem. Soc.* **1964**, *86*, 1166–1171.

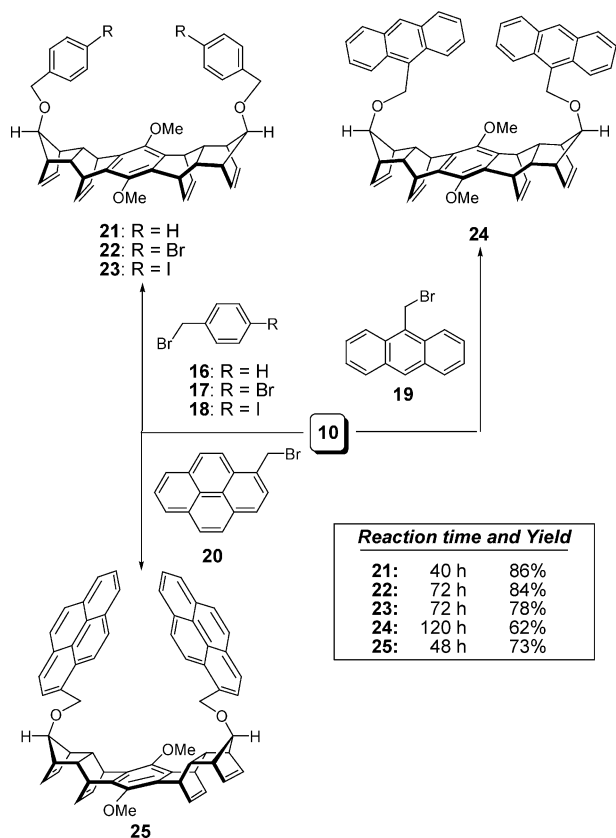
(22) (a) Lan, P.; Berta, D.; Porco, J. A., Jr.; South, M. S.; Parlow, J. *J. Org. Chem.* **2003**, *68*, 9678–9686. (b) Stack, D. E.; Hill, A. L.; Diffendaffer, C. B.; Burns, N. M. *Org. Lett.* **2002**, *4*, 4487–4490. (c) Akiyama, S.; Nakasuji, K.; Nakagawa, M. *Bull. Chem. Soc. Jpn.* **1971**, *44*, 2231–2236.

(23) (a) Okamoto, H.; Arai, T.; Sakuragi, H.; Tokumaru, K. *Bull. Chem. Soc. Jpn.* **1990**, *63*, 2881–2890. (b) Peck, R. M.; O'Connell, A. P. *J. Med. Chem.* **1972**, *15*, 68–70.

(24) (a) Ihmels, H.; Meiswinkel, A.; Mohrschladt, C. J.; Otto, D.; Waidelich, M.; Towler, M.; White, R.; Albrecht, M.; Schnurpfeil, A. *J. Org. Chem.* **2005**, *70*, 3929–3938. (b) Kaanumalle, L. S.; Gibb, C. L. D.; Gibb, B. C.; Ramamurthy, V. *J. Am. Chem. Soc.* **2005**, *127*, 3674–3675. (c) Frontera, A.; Orell, M.; Garau, C.; Quiñonero, D.; Molins, E.; Mata, I.; Morey, J. *Org. Lett.* **2005**, *7*, 1437–1440. (d) Yang, D.-D. H.; Yang, N. C.; Steele, I. M.; Li, H.; Ma, Y. Z.; Fleming, G. R. *J. Am. Chem. Soc.* **2003**, *125*, 5107–5110. (e) Kang, J.; Choi, M.; Kwon, J. Y.; Lee, E. Y.; Yoon, J. *J. Org. Chem.* **2002**, *67*, 4384–4386. (f) Ihmels, H.; Meiswinkel, A.; Mohrschladt, C. J. *Org. Lett.* **2000**, *2*, 2865–2867. (g) Wang, W.; Springsteen, G.; Gao, S.; Wang, B. *Chem. Commun.* **2000**, 1283–1284.

(25) (a) Takemura, H.; Nakamichi, H.; Sako, K. *Tetrahedron Lett.* **2005**, *46*, 2036–2066. (b) Kim, J. S.; Shon, O. J.; Rim, J. A.; Kim, S. K.; Yoon, J. *J. Org. Chem.* **2002**, *67*, 2348–2351. (c) Liao, J.-H.; Chen, C. T.; Fang, J.-M. *Org. Lett.* **2002**, *4*, 561–564.

**SCHEME 4. Bis-O-Alkylation of Tetraetheno-Bridged Dicyclopenta[*b,i*]anthracenediol 10 with Bromomethylarenes<sup>a</sup>**



<sup>a</sup> Reaction conditions: NaH (10 mmol), ArCH<sub>2</sub>Br (3 mmol), **10** (1 mmol), THF (30 mL), 45 °C.

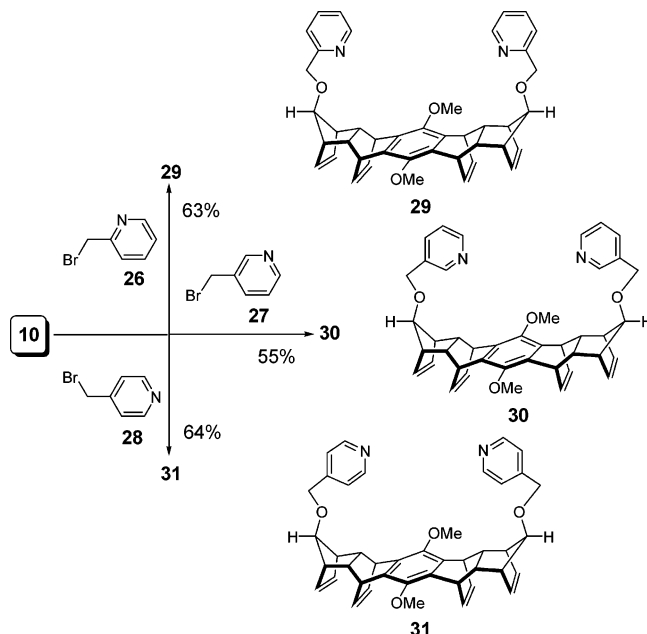
bis-pyridyl methyl ethers thereby attained are expected to act intramolecularly in a chelating mode, resembling the action of a pair of pincers, or intermolecularly as bridging ligands for the formation of either ring or chain compounds via coordination with metal ions.<sup>27</sup> Thus, the general procedure previously described for bis-O-alkylation of **10** with bromomethylarenes was followed, except that the amount of NaH was increased to 20 equiv because we used the hydrobromide salt of bromomethylpyridine. As shown in Scheme 5, the bis-O-alkylation of diol **10** with isomeric bromomethylpyridines (**26–28**) afforded the bis-pyridylmethyl crabs **29–31** in 63, 55, and 64%, respectively.

**<sup>1</sup>H NMR Analysis.** All the crab-like molecules **13–15**, **21–25**, and **29–31** gave satisfactory elemental

(26) (a) Petitjean, A.; Khoury, R. G.; Kyriysakas, N.; Lehn, J.-M. *J. Am. Chem. Soc.* **2004**, *126*, 6637–6647. (b) Holliday, B. J.; Farrell, J. R.; Mirkin, C. A. *J. Am. Chem. Soc.* **1999**, *121*, 6316–6317. (c) Munakata, M.; Zhong, J. C.; Kuroda-Sowa, T.; Maekawa, M.; Suenaga, Y.; Kasahara, M.; Konaka, H. *Inorg. Chem.* **2001**, *40*, 7087–7090. (d) Bilyk, A.; Harding, M. M.; Turner, P.; Hambley, T. W. *J. Chem. Soc., Dalton Trans.* **1994**, 2783–2790. (e) Wahl, P.; Krieger, C.; Schweitzer, D.; Staab, H. A. *Chem. Ber.* **1984**, *117*, 260–276.

(27) (a) Fujita, M.; Tomimiga, M.; Hori, A.; Therrien, B. *Acc. Chem. Res.* **2005**, *38*, 371–380. (b) Steel, P. J. *Acc. Chem. Res.* **2005**, *38*, 243–250. (c) Oh, M.; Stern, C. L.; Mirkin, C. A. *Inorg. Chem.* **2005**, *44*, 2647–2653. (d) Fujita, M. *Acc. Chem. Res.* **1999**, *32*, 53–61. (e) Hartshorn, C. M.; Steel, P. J. *Inorg. Chem.* **1996**, *35*, 6902–6903. (f) Suzuki, T.; Kotsuki, H.; Isobe, K.; Moriya, N.; Nakagawa, Y.; Ochi, M. *Inorg. Chem.* **1995**, *34*, 530–531.

**SCHEME 5. Bis-O-Alkylation of Tetraetheno-Bridged Dicyclopenta[*b,i*]anthracenediol 10 with Bromomethylpyridines<sup>a</sup>**



<sup>a</sup> Reaction conditions: NaH (20 mmol), PyCH<sub>2</sub>Br (3 mmol), **10** (1 mmol), THF (30 mL), 45 °C, 72 h.

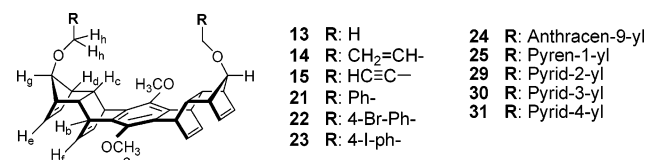


**FIGURE 4.** Labeling of the hydrogen atoms at the skeleton carbons of **13–15**, **21–25**, and **29–31**.

analytical or HRMS data, and were characterized by their spectral analyses (<sup>1</sup>H and <sup>13</sup>C NMR, IR, and MS). They showed relatively simple <sup>1</sup>H and <sup>13</sup>C NMR spectra, which indicated that they were symmetrical and their appended groups were conformationally mobile in solution. The assignments of the absorption signals for all hydrogen atoms at the main skeleton carbons of crab-like molecules were unequivocally made using chemical shift, <sup>1</sup>H–<sup>1</sup>H COSY, and HMQC experiments (Table S1, Supporting Information). A <sup>1</sup>H absorption signal (4H) appearing in the region between δ 4.0 and 5.4, which correlates with the <sup>13</sup>C line in the region between δ 63 and 70, is attributable to the –CH<sub>2</sub>–O– groups of appended units (H<sub>n</sub>, Figure 4). This <sup>1</sup>H signal, together with the characteristic absorption signals attributable to the hydrogens at vinyl and aromatic carbons, evidently signifies the attachments of allyl and arylmethyl groups to the polycyclic framework of diol **10**. The corresponding –CH<sub>2</sub>–O– groups of bis-propagyl ether **15** exhibited <sup>1</sup>H and <sup>13</sup>C absorption signals at δ 4.01 and 56.2, respectively. Bis-methyl ether **13** showed two <sup>1</sup>H singlets at δ 3.72 and 3.24, each with a relative intensity of 6H, that were due to the methoxy hydrogens at the central benzene ring and methano-bridge carbons, respectively. The chemical shift of the hydrogens in –CH<sub>2</sub>–O– groups (H<sub>n</sub>) increases from δ 3.24 for **13** to δ 5.42 for **24** and δ 5.13 for **25**, in



line with the expectation based on the combination of the  $-I$  effect and the anisotropic deshielding effect of  $\pi$ -electrons of multiple bonds and aromatic rings. The deshielding effect of anthracenyl rings in **24** appears to be most effective ( $\Delta\delta = 2.2$  ppm) followed by the pyrenyl rings in **25** ( $\Delta\delta = 1.9$  ppm). The hydrogens at the methano-bridge ( $H_g$ ) and ring junction ( $H_c$ ) carbons are also deshielded, although to a much smaller extent ( $\Delta\delta < 0.3$  ppm). When the chemical shifts of the remaining hydrogens ( $H_b$ ,  $H_d$ ,  $H_e$ , and  $H_f$ ) at the skeleton carbons and the methoxy hydrogens ( $H_a$ ) were compared with those of the respective hydrogens in bis-methyl ether **13**, only in the cases of **24** and **25** were any significant differences seen.

Most noticeable were the positions of the  $\text{CH}_3$  signals ( $H_a$ ) of the methoxy groups in **24** at  $\delta$  3.55 and in **25** at  $\delta$  3.40, which were shifted upfield by 0.17 and 0.32 ppm, respectively, relative to the position of **13** at  $\delta$  3.72. A plausible explanation suggested by the X-ray crystal structure of **25** (vide infra) would be that the  $\text{CH}_3$  substituents of the methoxy groups in **24** and **25** are located in the shielding zone of the large  $\pi$ -systems of the anthracenyl and pyrenyl rings to show signals ( $H_a$ ) at a higher field relative to that of **13** and other crab-like molecules with  $\pi$ -systems of smaller size. The hydrogens at aromatic rings of **24** and **25** displayed absorption signals at  $\delta$  7.32–8.35 and 7.87–8.21, respectively. When compared correspondingly with signals of aromatic hydrogens in 9-(methoxymethyl)anthracene ( $\delta$  7.47–8.47) and 1-(methoxymethyl)pyrene ( $\delta$  7.98–8.33),<sup>28</sup> the aromatic hydrogens in **24** and **25** exhibit upfield shifts of an average of 0.1 ppm. These observations suggest that the anthracenyl rings in **24** and the pyrenyl rings in **25** might align face to face in parallel fashion via an intramolecular  $\pi$ -stacking interaction, resulting in mutual shielding of aromatic hydrogens.

**Silver Complexes of Bis-Pyridylmethyl Crabs 29–31.** When a stoichiometric amount of an acetonitrile solution of silver salt ( $\text{AgNO}_3$ ,  $\text{AgBF}_4$ ,  $\text{AgCF}_3\text{SO}_3$ ,  $\text{AgClO}_4$ , or  $\text{AgPF}_6$ ) was mixed with a solution of bis-pyridylmethyl crab **29**, **30**, or **31** in  $\text{CH}_2\text{Cl}_2$  or THF, immediate precipitation occurred to give a very insoluble product that was difficult to purify by recrystallization. Thus, the reaction was performed by carefully adding an acetonitrile solution of silver salt into a  $\text{CH}_2\text{Cl}_2$  or THF solution of bis-pyridylmethyl crab and allowing the reaction to occur via slow diffusion between layers in the dark without disturbance. The precipitates that contained crystals were collected and washed with acetonitrile to remove intact silver salt, and from the reactions of **29** with  $\text{AgBF}_4$  and **30** with  $\text{AgNO}_3$  were furnished crystals suitable for a single-crystal X-ray structure determination. Complexation of the silver cation with pyridyl ligands was suggested by the  $^1\text{H}$  NMR spectra in  $\text{DMSO}-d_6$ , in which the resonance signals attributable to the pyridyl hydrogens appeared at lower fields than those of the corresponding hydrogens in bis-pyridylmethyl crabs **29**, **30**, and **31**. As revealed by the X-ray crystal structures (vide infra), the coordination mode depended on the location of the nitrogen atom in the pyridine ring relative to the appended position. For **29**, the bis-*o*-pyridylmethyl crab, a [2+2] dimeric dimetallo-cyclophane (**32**) was formed,

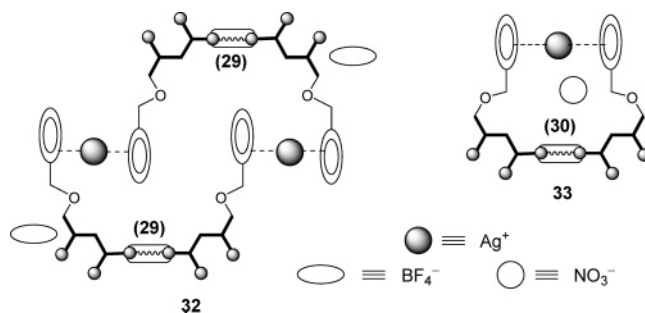


**FIGURE 5.** Schematic representations for the structures of the silver(I) complexes **32** and **33** from bis-*o*-pyridylmethyl and bis-*m*-pyridylmethyl crabs **29** and **30**.

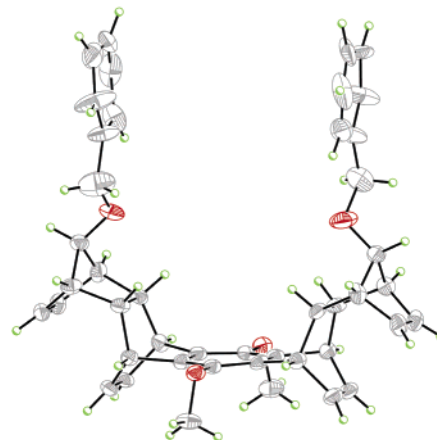


**FIGURE 6.** ORTEP drawing of molecular crab **21**. The thermal ellipsoids are drawn at the 30% level of probability. The two phenyl rings are disordered and separated by an inter-ring distance of about 7.3 Å.

and a [1+1] metallo-bridged cyclophane (**33**) was formed for the bis-*m*-pyridylmethyl crab **30**, in which the pyridyl ligands acted like the pair of pincers of a crab (Figure 5). A molecular model suggested that the bis-*p*-pyridylmethyl crab **31** would find it difficult to form a [1+1] Ag-bridged cyclophane similar to that of complex **33**, and it would be more likely to form a [2+2] silver-bridged cyclophane like that of **32**. Of course, multinuclear complexes in the form of oligomeric macrocycles or polymeric open-chain structures cannot be excluded, which for now precluded further verification.

**X-ray Crystal Structures of 21, 25, 32, and 33.** Among the crystals of all molecular crabs synthesized, only those obtained from **21** and **25** resulted in single crystals suitable for X-ray structure analysis. The selected interatomic distances and torsional angles observed in the solid-state structures of **EtOAc@6**, **21**, **25**, and **33** that describe the extent of folding of the molecular scaffold are listed in Table 1. When compared with the structure of **EtOAc@6** (Figure 3 and Table 1), the structure of **21** shown in Figure 6 reveals that the molecular scaffold is inward-folded unsymmetrically and to a larger extent ( $9.3$  vs  $5.1^\circ$ ), resulting in a shortening of the transannular distances between the oxygen atoms at methano-bridge carbons ( $\text{O1}-\text{O2}'$ , 7.06 Å), the carbon atoms of these methano-bridges ( $\text{C1}-\text{C1}'$ , 9.10 Å), and the carbon atoms of ring junctions ( $\text{C2}-\text{C2}'$ , 6.05 Å). The methyl groups of the dimethoxybenzene ring are oriented outward between two inner etheno-bridges, which are

(28) Yoshioka, N.; Andoh, C.; Kubo, K.; Igarashi, T.; Sakurai, T. *J. Chem. Soc., Perkin Trans. 2* **2001**, 1927–1932.

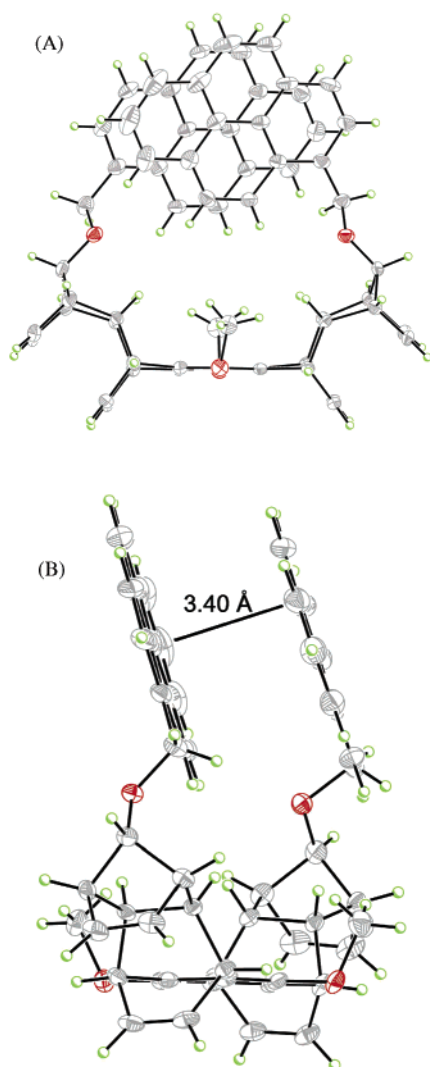


**FIGURE 7.** ORTEP drawings of the crystal structure of **25**; (A) face view, (B) side view, looking into the parallel alignment of pyrenyl rings. The thermal ellipsoids are drawn at the 30% level of probability.

separated by 6.96 Å, farther than that in **EtOAc@6**. The two appended phenyl rings in the room-temperature crystal structure of **21** were highly disordered. Nevertheless, the crystal structure of **21** reveals that the two phenyl rings are oriented perpendicular to the molecular platform with an inter-ring distance of about 7.3 Å, too great a distance for an intramolecular  $\pi$ - $\pi$  interaction. This structural feature may imply a similar situation in the crystal structures of other molecular crabs with  $\pi$ -systems of similar size.

Interestingly and differently from **21**, the solid-state structure of **25** displays a distinctive arrangement of its two pyrenyl rings (Figure 7a). In spite of their large size, these two pyrenyl rings twist across the concave side of the U-shaped molecular scaffold and align face to face in an antiparallel fashion. The two pyrenyl rings are nearly coplanar and separated by a shorter interatomic distance of about 3.40 Å (Figure 7b), similar to the interplanar distances in 2,7-dimethylpyrene (3.45 Å),<sup>29a</sup> [4.4]- and [3,3]-(2,7)pyrenophanes (3.48 Å),<sup>29b</sup> and graphite (3.35 Å). Although numerous examples of the face-to-face alignment of pyrenyl rings in proximity, either

intermolecular or intramolecular, have been identified in the literature with evidence from the solid-state structural<sup>26c-e</sup> or spectroscopic analysis,<sup>30</sup> the present case of **25**, to the best of our knowledge, may represent the first example of the solid-state structure of intramolecular  $\pi$ -stacking of pyrenyl rings that are self-assembled and separated by such a short distance without the assistance of either metal coordination<sup>26c,d</sup> or synthetically predestined arrangement.<sup>26e,29</sup> The two pyrenyl rings are estimated to have about 70% contact surface area, indicating the effective intramolecular  $\pi$ -stacking interaction between pyrenyl rings. Obviously, this arrangement of pyrenyl rings in **25** suggests that the two anthracenyl rings in molecular crab **24** could behave similarly, and the investigation of their luminescence properties should be informative regarding the  $\pi$ - $\pi$  interaction in **24** and **25**, the results of which will be presented in a later section. A minute difference in the shapes of the molecular platforms of **25** and **EtOAc@6** is revealed by the structure of **25** (Figure 7a) and Table 1. The molecular scaffold of **25** is inward-folded by a total of about 7.1°, nearly the same as that of **EtOAc@6** (5.1°). As a result, the transannular distances between the oxygen atoms at methano-bridge carbons (O1-O2'), the carbon atoms of these methano-bridges (C1-C1'), and the carbon atoms of ring junctions (C2-C2') in **25** are 7.57, 9.46, and 6.23 Å, respectively, close to those in **EtOAc@6**. Two inner etheno-bridges are separated by 6.83 Å, also very close to that in **EtOAc@6** (6.75 Å). Differently from that in **21**, the methyl groups of the dimethoxybenzene ring are oriented inward between two carbon atoms of ring junctions, reminiscent of the observed upfield-shifted <sup>1</sup>H resonance as a result of anisotropic shielding from pyrenyl rings (Table S1). The unit cell consists of a pair of enantiomeric molecules of **25**. They are aligned in head-to-head mode and displaced from one another in such a way to have a point of inversion (*S*<sub>2</sub>-symmetric). The intermolecular distance between pyrenyl rings is 9.5 Å, too far away to render an intermolecular  $\pi$ - $\pi$  interaction (Supporting Information).

The central dimethoxybenzene ring-containing platforms of the U-shaped molecular scaffolds in the [2+2] dimeric dimetallo-cyclophane **32** are nearly flat ( $\theta = 179.1^\circ/178.9^\circ$ , Table 1). The transannular distances between the oxygen atoms at methano-bridge carbons (O1-O2'), the carbon atoms of these methano-bridges (C1-C1'), and the carbon atoms of ring junctions (C2-C2') in each molecular scaffold of **32** are 7.77, 9.62, and 6.33 Å, respectively. Two inner etheno-bridges are separated by 6.75 Å, similar to that in **EtOAc@6**. As shown in the face and side views of the crystal structure of **32** (Figure 8), the two molecular crabs **29**, each carrying a

(29) (a) Irngartinger, H.; Kirrstetter, R. G. H.; Krieger, C.; Rodewald, H.; Staab, H. A. *Tetrahedron Lett.* **1977**, 1425–1429. (b) Staab, H. A.; Riegler, N.; Diederrich, F.; Krieger, C.; Schweitzer, D. *Chem. Ber.* **1984**, *117*, 246–259.

(30) (a) Moon, S.-Y.; Youn, N. J.; Park, S. M.; Chang, S.-K. *J. Org. Chem.* **2005**, *70*, 2394–2397. (b) Lee, J. Y.; Kim, S. K.; Jung, J. H.; Kim, J. S. *J. Org. Chem.* **2005**, *70*, 1463–1466. (c) Kim, S. K.; Lee, S. H.; Lee, J. Y.; Lee, J. Y.; Bartsch, R. A.; Kim, J. S. *J. Am. Chem. Soc.* **2004**, *126*, 16499–16506. (d) Nakahara, Y.; Toshiyuki Kida, T.; Nakatsuji, Y.; Akashi, M. *J. Org. Chem.* **2004**, *69*, 4403–4411. (e) Yuasa, H.; Miyagawa, N.; Izumi, T.; Nakatani, M.; Izumi, M.; Hashimoto, H. *Org. Lett.* **2004**, *6*, 1489–1492. (f) Nakahara, Y.; Matsumi, Y.; Zhang, W.; Kida, T.; Nakatsuji, Y.; Ikeda, I. *Org. Lett.* **2002**, *4*, 2641–2644. (g) Yang, J.-S.; Lin, C.-S.; Hwang, C.-Y. *Org. Lett.* **2001**, *3*, 889–892.



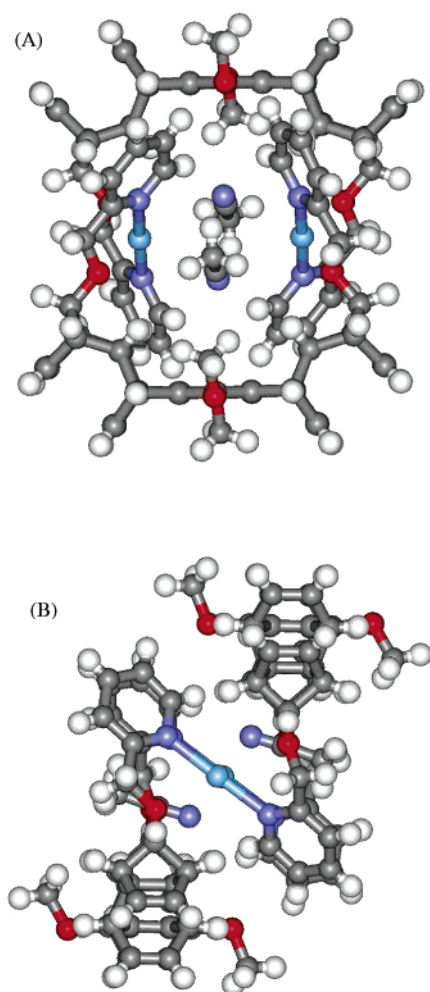


**FIGURE 8.** Ball-and-stick representations of the crystal structure of **32**; (a) face view, (b) side view. The Ag–N bond lengths are 2.18 and 2.19 Å. The N–Ag–N angle is 178.5°. The distance between the silver atoms is 5.41 Å. The counterions ( $\text{BF}_4^-$ ) are outside the circular structure, and have been omitted.

molecule of  $\text{CH}_3\text{CN}$  similar to that in **EtOAc@6** (Figure 3) and acting as a bis-monodentate ligand, are arranged head-to-head and offset such that two *o*-pyridyl rings, one from each crab, are paired and intermolecularly linked by  $\text{Ag}^+$  to form a circular, centrosymmetric structure. The distance between the silver atoms is 5.41 Å, longer than the sum of the Ag–Ag van der Waals radii (3.44 Å).<sup>31</sup> The Ag–N bond lengths are 2.18 and 2.19 Å, and the N–Ag–N angle is 178.5°, indicative of a normal coordination of the Ag ion with two nitrogen atoms from two distinct pyridyl ligands. The Ag ion is not coordinated with either of the nitrogen atoms from the two  $\text{CH}_3\text{CN}$  molecules, as they are incorrectly aligned and separated by 3.25 and 3.55 Å. The two Ag-linked pyridyl rings are not coplanar; the C–N–(Ag)–N'–C' torsional angle is 74.0°.

The bis-*m*-pyridylmethyl molecular crab **30** acts as a bidentate ligand to coordinate a silver cation to form a [1+1] metallo-bridged cyclophane **33**. The solid-state structure is depicted in Figure 9, and the selected

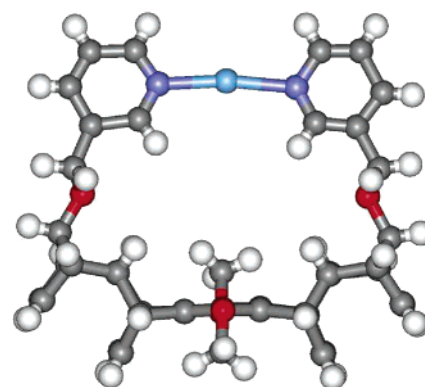


**FIGURE 9.** Ball-and-stick representations of the crystal structure of **33**. The distance from the Ag atom to the dimethoxybenzene ring is 7.26 Å. The Ag–N bond length is averaged to be 2.18 Å. The N–Ag–N angle is 172.3°. The counterion ( $\text{NO}_3^-$ ) is outside the cavity, and has been omitted.

interatomic distances and torsional angles are listed in Table 1. Perhaps, because of intramolecular complexation, the U-shaped molecular scaffold in **33** is stretched out, and hence outward-folded unsymmetrically by a total of about 7.6°, resulting in a lengthening of the transannular distances between the oxygen atoms at methano-bridge carbons (O1–O2', 8.98 Å), the carbon atoms of these methano-bridges (C1–C1', 10.41 Å), and the carbon atoms of ring junctions (C2–C2', 6.68 Å). The two methyl groups of the dimethoxybenzene ring are oriented trans to each other between two inner etheno-bridges, which are separated by 6.37 Å, the shortest distance among those observed in the solid-state (A) structures of molecular crabs (Table 1). The distance between the Ag atom and the dimethoxybenzene ring is 7.26 Å. The Ag ion is normally bi-coordinated with two nitrogen atoms from each of the pyridyl ligands by a N–Ag–N angle of 172.3° (endocyclic). As in **32**, the Ag–N bond length is averaged to be 2.18 Å. However, differently from **32**, the two Ag-linked pyridyl rings are nearly coplanar; the C–N–(Ag)–N'–C' torsional angle is 178.7°.

**Luminescence Properties of Molecular Crabs 24 and 25.** In cyclohexane, the bis-pyrenyl crab **25** exhibits an  $S_0 \rightarrow S_1$  ( $\pi \rightarrow \pi^*$ ) absorption maximized at 345 nm, broadened and red-shifted by about 10 nm as compared to that of pyrene (335 nm).<sup>32</sup> When **25** in solid state or in solution ( $\text{CH}_2\text{Cl}_2$ ), which is colorless, was illuminated by a light of  $\lambda = 365$  nm, it emitted blue-colored light, a phenomenon reflecting the effective intramolecular  $\pi$ -stacking of pyrenyl rings as shown in the X-ray crystal structure of **25**. In solution, the fluorescence spectrum ( $\text{CH}_2\text{Cl}_2$ ,  $\lambda_{\text{ex}} = 345$  nm) of **25** at room temperature exhibits characteristic monomer emissions of pyrene around 375–400 nm,<sup>3e</sup> followed by a very broad, structureless, and strongly red-shifted "excimer" emission around 465 nm. Obviously, **25** in solution exists on average in conformations of the two pyrenyl units situated in proximity, allowing an intramolecular excimer state to be reached upon excitation. The intramolecular nature of excimer formation, as a result of the steric

(31) Bondi, A. J. *Phys. Chem.* **1964**, *68*, 441–451.

(32) (a) Du, H.; Fuh, R. A.; Li, J.; Corkan, A.; Lindsey, J. S. *Photochem. Photobiol.* **1998**, *68*, 141–142. (b) Berlman, I. B. *Handbook of Fluorescence Spectra of Aromatic Molecules*; Academic Press: New York, 1971.

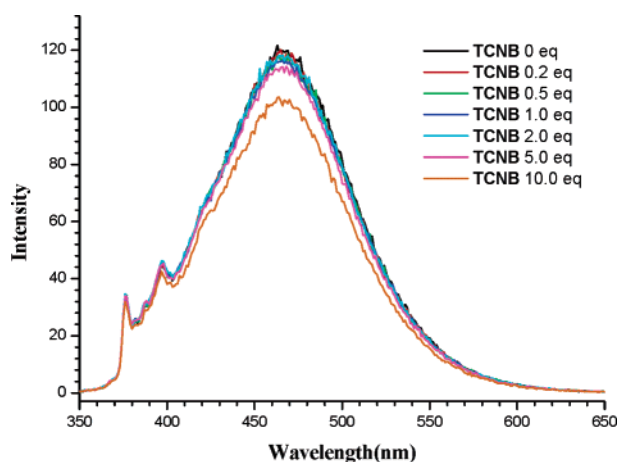


**FIGURE 10.** Room-temperature fluorescence spectra of **25** in the presence of different equivalents of TCNB in a dichloromethane solution.  $[\mathbf{25}] = 1.0 \times 10^{-5}$  M.  $\lambda_{\text{ex}} = 345$  nm.

arrangement of pyrenyl units best illustrated in the X-ray crystal structure of **25** (Figure 7), was suggested by the observation of the unchanged wavelength of the fluorescence spectra upon changing the concentration of **25** (Supporting Information). In the presence of electron-deficient 1,4-dinitrobenzene (DNB) or 1,2,4,5-tetracyanobenzene (TCNB), the intensity of both monomer and excimer emissions was not significantly changed. As shown in Figure 10, the fluorescence spectrum of **25** in  $\text{CH}_2\text{Cl}_2$  ( $1.0 \times 10^{-5}$  M) remains essentially unchanged upon addition of TCNB up to about 10 equiv. Beyond this point, the intensity of fluorescence of both monomer and excimer begins to decrease significantly, presumably as a result of diffusion quenching (panel 9b of Figure S17 in the Supporting Information). This observation suggests that the intramolecular  $\pi$ - $\pi$  interaction of pyrenyl rings in **25** is strong, and hence prevents the excimer emission from quenching by formation of a host-guest complex with electron-deficient species.<sup>33</sup>

With reference to anthracene, the bis-anthracenyl crab **24** in  $\text{CH}_2\text{Cl}_2$  exhibits a similar UV absorption spectrum and a fluorescence spectrum ( $\lambda_{\text{ex}} = 258$  nm) that is similar in band shape but with  $\lambda_{\text{max}}$ 's red-shifted by 10–12 nm (392, 415, and 439 nm and a shoulder 468 nm). Similar to that of bis-pyrenyl crab **25**, the fluorescence  $\lambda_{\text{max}}$  of **24** was not changed with a change in the concentration, indicating that the red-shift fluorescence is the result of the formation of an excimer between the two anthracenyl rings in **24**.<sup>24</sup> When **24** was excited at  $\lambda_{\text{ex}} = 387$  nm, the intensity and band shape of fluorescence emission were not affected upon the addition of electron-deficient TCNB (0.5–450 equiv) as shown in Figure 11. These luminescence properties of **24**, together with the similar shielding effect observed for the aromatic hydrogens of **24** and **25**, suggest that the two anthracenyl rings in **24** also align face to face to form an intramolecular excimer via the  $\pi$ - $\pi$  interaction, which appears to provide resistance to being quenched by the formation of a host-guest complex with electron-deficient species.<sup>33</sup>

(33) Formation of a host-guest complex with electron-deficient species was not indicated for either **24** or **25** by their  $^1\text{H}$  NMR spectra, which were not changed upon the addition of DNB and TCNB.

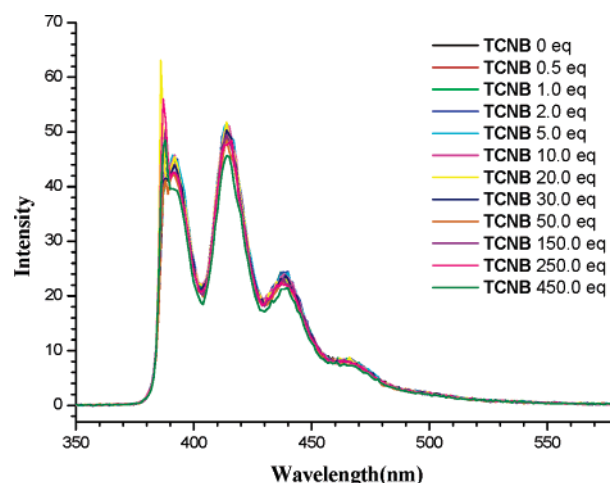


**FIGURE 11.** Room-temperature fluorescence spectra of **24** in the presence of different equivalents of TCNB in a dichloromethane solution.  $[\mathbf{24}] = 1.0 \times 10^{-5}$  M.  $\lambda_{\text{ex}} = 387$  nm.

## Conclusion

We have successfully synthesized a unique U-shaped, multifunctionalized platform molecule **10**, and established practicability of functionalization via bis-*O*-alkylation of its two terminally located endo-oriented hydroxyl groups using the protocol of Williamson ether synthesis. Functionalization resembling the attachment of the pair of pincers of a crab led to the crab-like molecules that demonstrated pincer-like action as, for example, in the complexation of bis-*m*-pyridyl crab **30** with silver ion to form a [1+1] metallo-bridged cyclophane **33**. For bis-*o*-pyridyl crab **29**, the silver(I) complex was found to be a [2+2] dimeric dimetallo-cyclophane **32**. Two pyrenyl rings in **25** encounter strong arene-arene interactions resulting in the self-assembled intramolecular  $\pi$ -stacking, separated by 3.40 Å as revealed by its solid-state structure, and consequently formed an excimer responsible for the emission around 465 nm, which could not be quenched by electron-deficient species, such as DNB and TCNB. Similarly, the two anthracenyl rings in molecular crab **24** also exhibited  $\pi$ - $\pi$  interaction, as revealed by its red-shifted fluorescence that was not quenched by electron-deficient species. The preliminary conclusion concerning the formation of intramolecular excimers of **24** and **25**, which provide resistance to quenching, requires future kinetic studies to verify. Further application of platform molecule **10** for functionalized polycyclic molecules of specially designed architecture is in progress.

**Acknowledgment.** The financial support from the National Science Council of Taiwan (NSC90-2113-M-194-014) is gratefully acknowledged. Partial financial support from the Academia Sinica of Taiwan is also acknowledged.

**Supporting Information Available:** Experimental Section:  $^1\text{H}$  chemical shift data for **13**–**15**, **21**–**25**, and **29**–**31** (Table S1); crystal data and structure refinement for **EtOAc@6** and **25** (Table S2–S6);  $^1\text{H}$  spectra of **6**, **10**, **11**, **24**, and **25**;  $^{13}\text{C}$  NMR, DEPT, COSY, and HMQC spectra of **10**; COSY spectra of **21**, **24**, **25**, and **29**–**31**; crystal packing of **EtOAc@6** and **25**; and room-temperature UV and fluorescence spectra of **24** and **25**. This material is available free of charge via the Internet at <http://pubs.acs.org>

JO051006F